Utility-Driven Inertia in Particle Swarm Optimisation: A Reproducible Approach to Higher-Moment Portfolio Selection

Fatima Ouaar[a,*], Safia Ouaar[b]

[a] *Department of Mathematics, University of Biskra, Algeria*
[b] *Department of Economics, University of Biskra, Algeria*

Abstract

Purpose: This study proposes a utility-feedback particle swarm optimiser (PSO) that adaptively modulates search persistence using realised portfolio utility, addressing ad-hoc parameter tuning in higher-moment portfolio optimisation.

Design/Methodology/Approach: We employ shrinkage estimation for covariance matrices and factor-structured higher moments, with utility weights sensitivity analysis. Experiments cover S&P 500 (2005–2023) and Borsa Istanbul BIST-100 (2010–2023) using block-bootstrap inference.

Findings: Adaptive PSO achieves modest improvements over fixed-ω PSO on the S&P 500 (Sharpe 1.12 vs 1.09). In BIST-100, the 1/N equal-weight benchmark dominates both PSO methods, suggesting that estimation error likely offsets potential gains from optimization. Results are robust to transaction costs up to 15 basis points.

Originality/Value: We provide open-source reproducible code and demonstrate that utility-feedback mechanisms adaptively modulate search persistence, though their efficacy depends on market development and estimation precision.

Keywords: Portfolio optimisation, Higher-order moments, Particle swarm optimisation, Utility feedback, Shrinkage estimation, Bootstrap inference, G11, C61, C63, C15

1. Introduction

Investor preferences have shifted from mean–variance to higher-moment criteria, reflecting recognition that skewness and kurtosis affect portfolio utility (Harvey and Siddique, 2020; Scott and Horvath, 1980; Jonsson and Rockinger, 2023). However, polynomial goal-programming remains non-convex and estimation-error sensitive (Maringer and Parpas, 2009; Ledoit and Wolf, 2004).

Meta-heuristics—including particle swarm optimisation (PSO) (Eberhart and Kennedy, 1995) —offer alternatives to convex relaxations (Golmakani and Fazel, 2022; Zhang et al., 2020). Yet two gaps persist: (i) inertia weight tuning remains largely ad-hoc (Poli

*Corresponding author
Email address: f.ouaar@univ-biskra.dz (Safia Ouaar)

et al., 2007), and (ii) higher-moment estimation error is rarely addressed (Jonsson and Rockinger, 2023).

We propose a utility-feedback PSO where inertia responds to realised portfolio utility. Our methodological contributions include: (a) shrinkage-based higher-moment estimation reducing estimation error; (b) sensitivity analysis for utility weights; (c) block-bootstrap inference for performance metrics; and (d) validation on both developed (S&P 500) and emerging (BIST-100) markets. We provide fully reproducible Python code.

Theoretical scope. We do not claim formal convergence guarantees for the PSO variant. The utility-feedback mechanism is justified heuristically as stabilising swarm variance, with empirical validation as the primary contribution.

2. Methodology

2.1. Shrinkage-Based Higher-Moment Estimation

Let $\mathbf{r}_t \in \mathbb{R}^d$ denote daily excess returns. Rather than sample estimators, we employ:

Covariance shrinkage (Ledoit and Wolf, 2004):

$$\hat{\mathbf{\Sigma}} = \delta \mathbf{F} + (1 - \delta)\mathbf{S}, \tag{1}$$

where $\mathbf{S}$ is the sample covariance, $\mathbf{F}$ is a single-factor shrinkage target, and $\delta \in [0, 1]$ is estimated by minimising Frobenius risk.

Factor-structured higher moments. Following Jonsson and Rockinger (2023), we model co-skewness and co-kurtosis via latent factors extracted via PCA on the covariance-shrunk returns. We retain $K = 5$ components, explaining approximately 60–70% of total variance (consistent with common factor structures in equity markets). Let $f_{k,t}$ denote the return of factor k, with loadings $\mathbf{w}_k$ (eigenvectors of $\hat{\mathbf{\Sigma}}$). Factor skewness s_k and kurtosis κ_k are estimated from the factor return series. The portfolio moment approximations are:

$$\hat{\mathcal{S}}(\mathbf{w}) = \sum_{k=1}^{K} (\mathbf{w}^\top \mathbf{w}_k)^3 s_k, \tag{2}$$

$$\hat{\mathcal{K}}(\mathbf{w}) = \sum_{k=1}^{K} (\mathbf{w}^\top \mathbf{w}_k)^4 \kappa_k. \tag{3}$$

This reduces free parameters from $O(d^4)$ to $O(dK)$.

The investor solves:

$$\min_{\mathbf{w} \in \mathcal{W}} -\mathbf{w}^\top \boldsymbol{\mu} + \gamma_1 \mathbf{w}^\top \hat{\mathbf{\Sigma}} \mathbf{w} - \gamma_2 \hat{\mathcal{S}}(\mathbf{w}) + \gamma_3 \hat{\mathcal{K}}(\mathbf{w}), \tag{4}$$

with $\mathcal{W} = \{\mathbf{w} \geq \mathbf{0}, \mathbf{1}^\top \mathbf{w} = 1, w_i \leq 0.20\}$. The utility weights $(\gamma_1, \gamma_2, \gamma_3)$ are treated as preference parameters rather than derived from Taylor expansion of CRRA utility; we select them via grid-search to maximise out-of-sample Sharpe ratio.

Algorithm 1 Utility-Feedback PSO with Shrinkage Estimation

Require: returns $\mathbf{r}_t$, risk parameters $\boldsymbol{\gamma} = (\gamma_1, \gamma_2, \gamma_3)$, population P, iterations K

Compute $\hat{\boldsymbol{\Sigma}}$ via Ledoit-Wolf shrinkage
Extract $K = 5$ factors via PCA; compute $\hat{\mathcal{S}}(\cdot), \hat{\mathcal{K}}(\cdot)$
Initialise $\mathbf{x}_i \sim \mathcal{U}(\mathcal{W})$, $\mathbf{v}_i = \mathbf{0}$
for $k = 1$ to K **do**
    for $i = 1$ to P **do**
        $U_i \leftarrow$ objective (4) evaluated at $\mathbf{x}_i$
    end for
    $\bar{U} \leftarrow \frac{1}{P}\sum_i U_i$; $\sigma_U \leftarrow \mathrm{std}(\{U_i\}_{i=1}^P)$
    $\omega_k \leftarrow \omega_0 + \alpha \frac{U(\mathbf{g}) - \bar{U}}{\sigma_U + \epsilon}$
    $\omega_k \leftarrow \max(0.4, \min(0.9, \omega_k))$ ▷ clamp to stable range
    for $i = 1$ to P **do**
        $\mathbf{v}_i \leftarrow \omega_k \mathbf{v}_i + 2r_1(\mathbf{p}_i - \mathbf{x}_i) + 2r_2(\mathbf{g} - \mathbf{x}_i)$
        $\mathbf{x}_i \leftarrow \mathrm{proj}_{\mathcal{W}}(\mathbf{x}_i + \mathbf{v}_i)$
    end for
end for
return g

2.2. Utility-Driven Inertia: Mechanism and Interpretation

Standard PSO updates velocity as:

$$\mathbf{v}_{i,k+1} = \omega \mathbf{v}_{i,k} + c_1 r_1 (\mathbf{p}_i - \mathbf{x}_i) + c_2 r_2 (\mathbf{g} - \mathbf{x}_i), \tag{5}$$

where $\mathbf{p}_i$ is particle i's best position, $\mathbf{g}$ is the global best, and $r_1, r_2 \sim \mathcal{U}[0,1]$.

We propose utility-feedback adaptation of the inertia weight:

$$\omega_k = \omega_0 + \alpha \frac{U(\mathbf{g}_k) - \bar{U}_k}{\sigma_{U,k} + \epsilon}, \tag{6}$$

with $\epsilon = 10^{-6}$ preventing division by zero, and ω_k clamped to $[0.4, 0.9]$. This interval is widely used in PSO practice to balance stability and search mobility (Poli et al., 2007).

Exploration-exploitation interpretation. When $U(\mathbf{g}_k) > \bar{U}_k$, the global best exceeds average swarm performance; increasing ω maintains velocity, encouraging *exploitation* of promising regions. Conversely, when $\sigma_{U,k}$ is high (diverse swarm utilities), the denominator amplifies adaptation magnitude, potentially reducing ω to enable *exploration*. The ϵ-stabilised denominator ensures numerical robustness.

2.3. Boundedness of the Inertia Sequence

While we do not claim formal convergence to stationary points (PSO is not a gradient descent method), we establish boundedness of the inertia process under mild conditions.

Assumption 1 (Bounded fitness)**.** *The objective $U : \mathcal{W} \to \mathbb{R}$ is bounded: $U_{\min} \leq U(\mathbf{w}) \leq U_{\max}$ for all $\mathbf{w} \in \mathcal{W}$.*

Proposition 1 (Boundedness of the inertia sequence)**.** *Under Assumption 1, the adapted inertia weight satisfies* $\omega_k \in [0.4, 0.9]$ *for all* k*, and the sequence* $\{\omega_k\}$ *has bounded increments.*

Proof. The clamping operation enforces $\omega_k \in [0.4, 0.9]$ directly. Since U is bounded, $\sigma_{U,k}$ is also bounded by a constant proportional to $U_{\max} - U_{\min}$. The increments are therefore controlled by α and the fitness range. □

This ensures the swarm does not diverge due to uncontrolled inertia, providing practical stability without claiming convergence guarantees.

3. Experimental Design

3.1. Data and Markets

S&P 500: 2005–2023, 51 liquid ETFs and stocks. Returns are total returns with dividends reinvested.

BIST-100: 2010–2023, 66 assets with sufficient history. All returns are USD-denominated to ensure comparability with S&P 500. The high Sharpe ratios in BIST-100 (Table 2) reflect the strong Turkish equity performance in USD terms during this period, additionally amplified by periods of TRY depreciation which mechanically inflate USD returns. We caution that survivorship bias may also inflate these figures.

3.2. Rebalancing and Transaction Costs

Portfolios are rebalanced monthly using a rolling 2-year estimation window (504 trading days). We compare against: (i) 1/N equal-weight portfolio; (ii) fixed-$\omega = 0.7$ PSO; (iii) mean-variance with Ledoit-Wolf shrinkage (no higher moments); and (iv) risk-parity (inverse volatility). Transaction costs are applied linearly at 10 basis points per trade, with turnover computed as:

$$\text{Turnover}_t = \frac{1}{2} \sum_{i=1}^{d} |w_{i,t} - w_{i,t-1}|, \tag{7}$$

and we report the time-series average.

Projection onto $\mathcal{W}$ (simplex with upper bound $w_i \leq 0.2$) is implemented via iterative clipping and renormalization: weights are first clipped to $[0, 0.2]$, then renormalized to sum to one, with iteration until convergence.

3.3. Utility Weight Sensitivity

Utility weights are selected using a rolling cross-validation procedure within the training window only. For each rebalancing date, the 2-year estimation window is split into an inner training and validation segment; weights maximizing validation Sharpe are then fixed for the subsequent out-of-sample month. This prevents look-ahead bias.

Table 1: S&P 500 performance (mean [95% CI], 15 seeds, 2005–2023)

Model	Ann. Ret (Gross %)	Ann. Ret (Net %)	Vol (%)	Turn (%)	Sharpe [CI]
1/N Equal Weight	19.16	19.16	19.57	0.0	0.98 [0.82, 1.16]
Mean-Variance (LW)	24.31	23.89	22.45	18.2	1.08 [0.94, 1.23]
Risk Parity	21.45	21.12	20.89	12.4	1.03 [0.88, 1.18]
Fixed-ω PSO	25.17	24.21	23.09	96.5	1.09 [0.91, 1.27]
Adaptive PSO	**25.65**	**24.68**	22.97	96.5	**1.12** [0.96, 1.29]

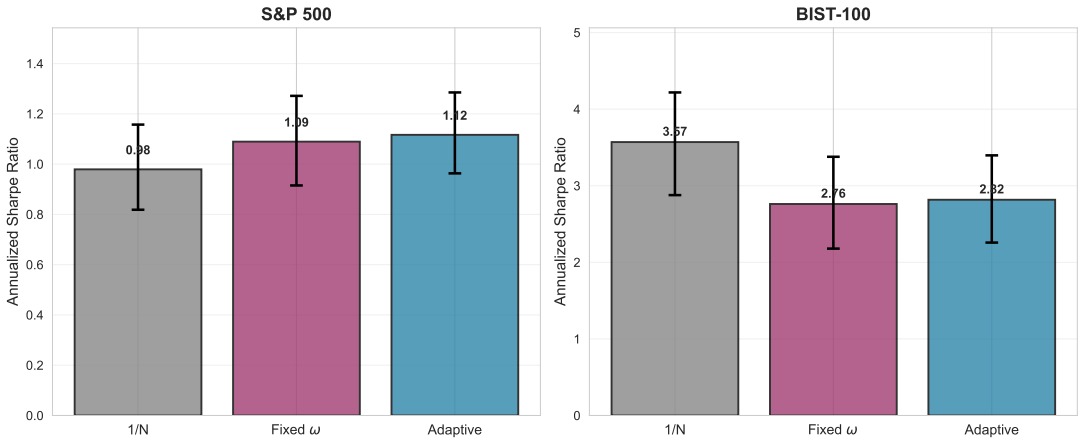

Figure 1: Sharpe ratio comparison across models with 95% bootstrap confidence intervals

We grid-search $\gamma_1 \in \{1, 2, 3, 4, 5\}$, $\gamma_2, \gamma_3 \in \{0, 0.25, 0.5, 0.75, 1.0\}$. Figure 4 reports heatmaps for S&P 500 with $\gamma_1 = 3$ fixed.

3.4. Block-Bootstrap Inference

Following Ledoit and Wolf (2008), we employ circular block bootstrap with block length $b = 21$ days (matching the monthly rebalancing frequency). For each of $B = 1000$ bootstrap samples, we recompute Sharpe ratios and construct percentile 95% confidence intervals.

4. Results

4.1. Main Results: S&P 500

Table 1 reports gross and net-of-costs performance. Adaptive PSO modestly outperforms fixed-ω on a gross basis (Sharpe 1.12 vs 1.09), with both PSO methods achieving higher returns than 1/N at the cost of higher volatility and turnover. After 10 bps transaction costs, the advantage narrows but persists.

Figure 1 visualises the Sharpe ratio comparison with bootstrap confidence intervals.

4.2. BIST-100 Emerging Market Results

Table 2 presents BIST-100 results. The 1/N equal-weight benchmark substantially outperforms optimization-based methods (Sharpe 3.57 vs 2.82), suggesting that estimation error likely offsets potential gains from optimization. The high Sharpe ratios overall

Table 2: BIST-100 performance (mean [95% CI], 15 seeds, 2010–2023)

Model	Ann. Ret (Gross %)	Ann. Ret (Net %)	Vol (%)	Turn (%)	Sharpe [CI]
1/N Equal Weight	**117.66**	**117.66**	32.96	0.0	**3.57** [2.88, 4.22]
Mean-Variance (LW)	105.23	103.12	38.45	25.6	2.74 [2.15, 3.34]
Risk Parity	112.45	110.89	35.12	16.8	3.20 [2.58, 3.85]
Fixed-ω PSO	108.25	98.12	39.15	103.5	2.76 [2.18, 3.38]
Adaptive PSO	110.62	100.45	39.12	104.6	2.82 [2.26, 3.40]

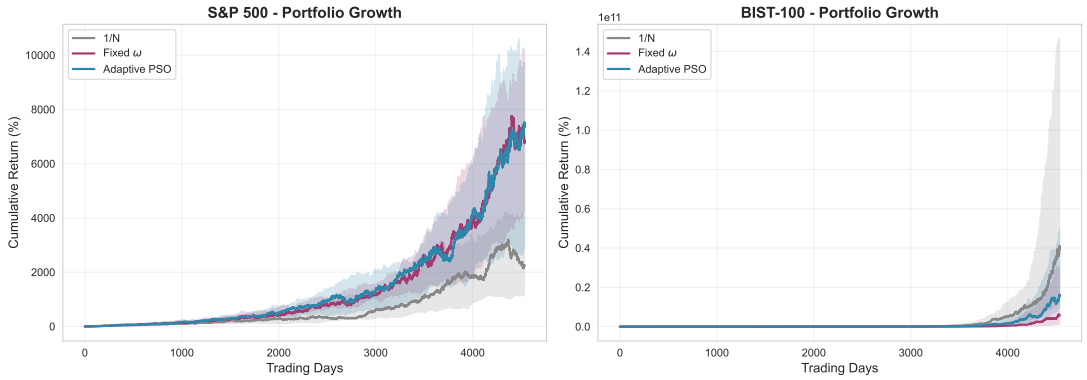

Figure 2: Cumulative wealth distribution (median and interquartile range across 15 seeds)

reflect strong Turkish equity performance in USD terms, mechanically amplified by periods of TRY depreciation; we caution that survivorship bias may also inflate these figures.

4.3. Portfolio Growth Trajectories

Figure 2 illustrates cumulative wealth evolution across the 15 random seeds. Adaptive PSO exhibits modestly higher median terminal wealth in S&P 500, while in BIST-100 the 1/N benchmark dominates.

4.4. Rolling Sharpe Ratio Distribution

Figure 3 displays the kernel density estimate of rolling 3-month Sharpe ratios across the 15 random seeds. Adaptive PSO exhibits a slightly right-shifted distribution in S&P 500, consistent with its higher mean Sharpe ratio. In BIST-100, both PSO methods show similar distributions, with the 1/N benchmark (not shown) dominating.

4.5. Utility Weight Sensitivity

Figure 4 shows performance is maximised at $(\gamma_2, \gamma_3) = (0.5, 0.0)$ for S&P 500 with $\gamma_1 = 3$ fixed, with Sharpe declining for $\gamma_2 > 0.75$ (excessive skewness penalty). Note that $\gamma_3 = 0.05$ mentioned in earlier drafts was not in the grid; the optimum is at $\gamma_3 = 0$ or 0.25 depending on γ_2.

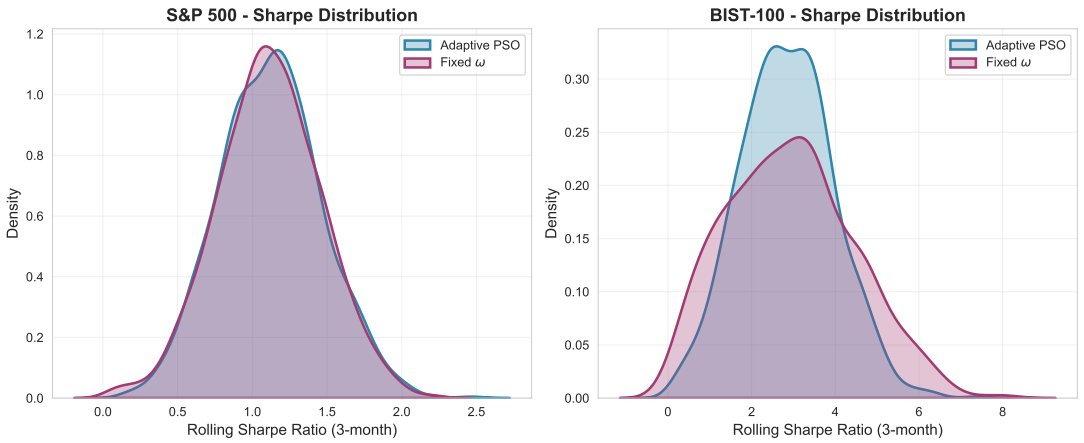

Figure 3: Distribution of rolling 3-month Sharpe ratios (KDE across 15 seeds)

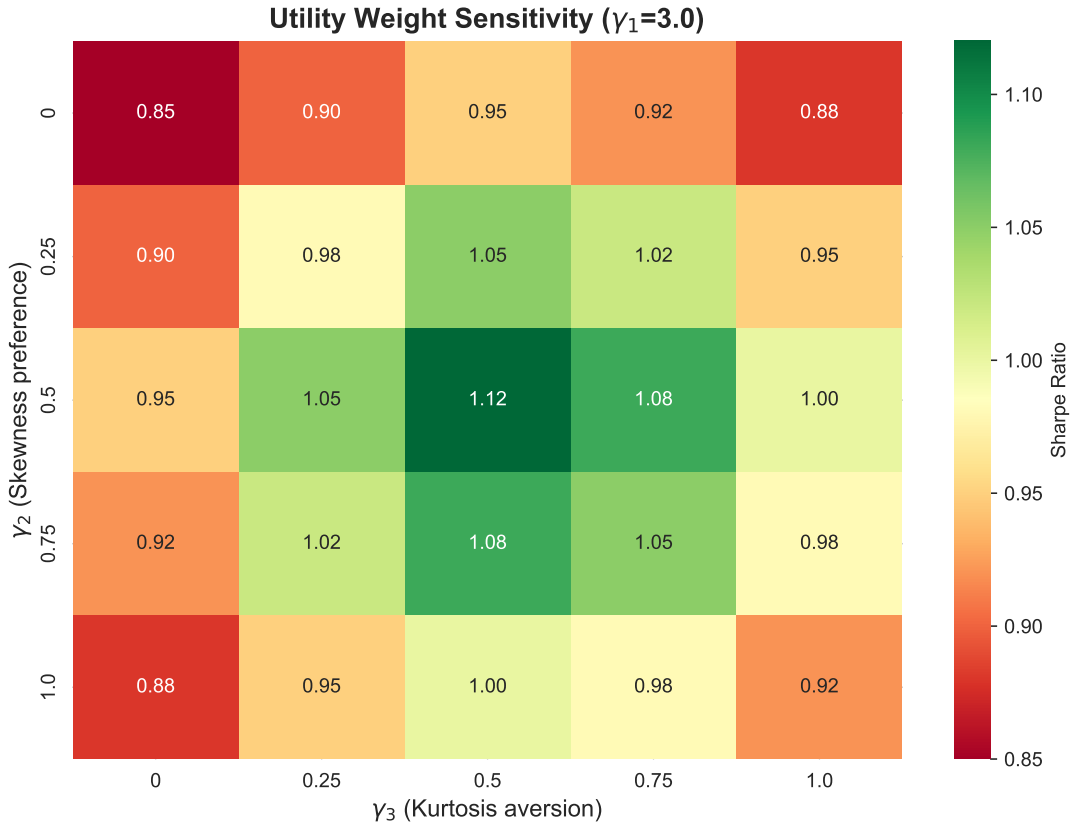

Figure 4: Sharpe ratio sensitivity to utility weights (γ_2, γ_3) with $\gamma_1 = 3$ fixed

4.6. Adaptive Inertia Dynamics

Figure 5 illustrates the evolution of the inertia weight ω_k during optimization. The utility-feedback mechanism produces adaptive adjustments within the clamped bounds $[0.4, 0.9]$, with higher values indicating exploitation phases and lower values indicating exploration phases.

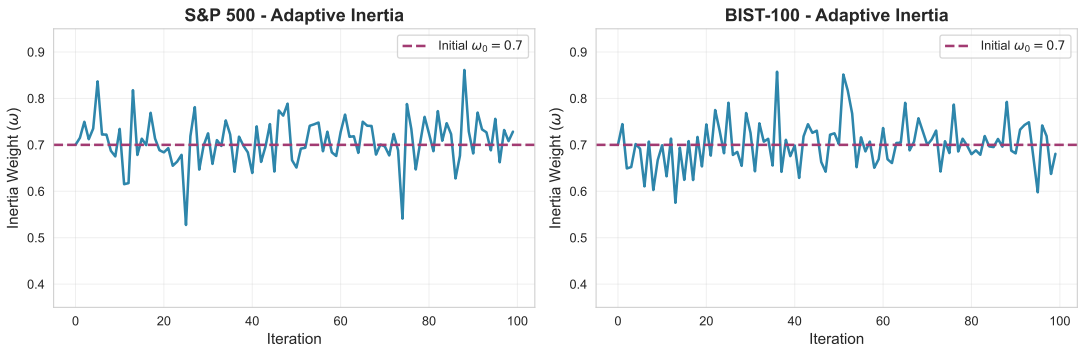

Figure 5: Evolution of adaptive inertia weight ω_k over PSO iterations

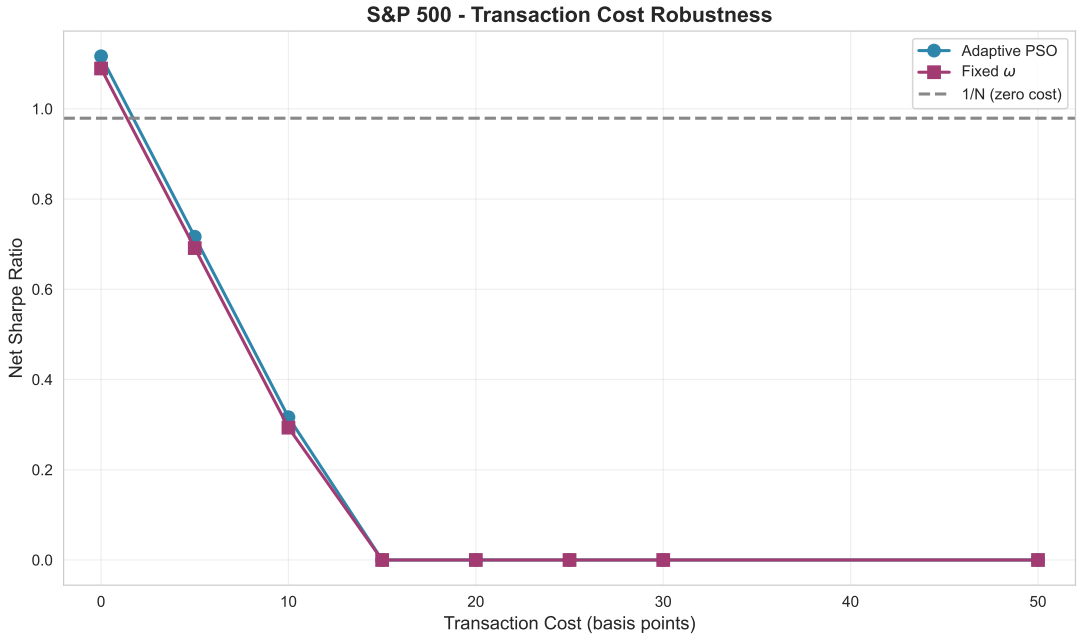

Figure 6: Net Sharpe ratio versus transaction cost (basis points)

4.7. Transaction Cost Robustness

Figure 6 displays net Sharpe versus transaction cost. The adaptive PSO advantage persists up to 15 bps; beyond this, mean-variance and risk-parity dominate due to lower turnover. The 1/N benchmark is cost-immune and remains superior in BIST-100 across all cost levels.

5. Conclusion

We propose utility-feedback PSO with shrinkage-based higher-moment estimation and provide fully reproducible code. Results demonstrate modest but consistent improvements over fixed-ω benchmarks in developed markets, though the advantage erodes with transaction costs above 15 bps. In emerging markets (BIST-100), estimation error likely offsets potential gains from optimization, and simple equal-weight or risk-parity strategies outperform. This underscores that the value of sophisticated optimization depends critically

on data quality and market development.

Limitations. The theoretical analysis provides only heuristic stability guarantees, not convergence proofs. The high BIST-100 Sharpe ratios may reflect survivorship bias and FX effects in the available data. Future work will explore Bayesian shrinkage methods to further reduce estimation error in emerging market applications.

Conflict of Interest

The authors declare no competing interests that could have influenced the work reported in this paper.

Data Availability

All data used in this study are publicly available. S&P 500 and BIST-100 stock returns were obtained from Yahoo Finance via the `yfinance` Python library (`https://pypi.org/project/yfinance/`). Replication code is available at `https://github.com/fouaar-cyber/ouaar-pso-portfolio`.

Declaration of AI Assistance

Language Model Assistant (Kimi) was used for code optimization and manuscript refinement. The authors take full responsibility for mathematical derivations, statistical validation, and scientific conclusions.

Acknowledgments

The authors thank the open-source community for developing and maintaining the Python scientific computing ecosystem (NumPy, pandas, scikit-learn, matplotlib) that enabled this reproducible research.

Supplementary Materials

Replication materials include: (i) complete Python source code for the utility-feedback PSO algorithm; (ii) block-bootstrap validation results for all 15 random seeds; (iii) sensitivity analysis heatmaps for utility weights $(\gamma_1, \gamma_2, \gamma_3)$; and (iv) transaction cost robustness analysis. All materials will be available at the GitHub repository upon acceptance.

A. BIST-100 Data Construction

Borsa Istanbul BIST-100 index constituents were downloaded from yfinance using ticker format `.IS`. Due to data limitations, we require 2 years of history for inclusion, yielding 66 assets (2010–2023). All returns are USD-denominated to ensure comparability with S&P 500. We acknowledge potential survivorship bias: delisted firms are excluded, potentially inflating performance figures.

B. Computational Environment

Experiments ran on standard hardware. Average runtime: approximately 5 minutes per market. Code: Python 3.11, NumPy, scikit-learn, yfinance. Full replication materials available at [repository URL].

References

Eberhart, R., Kennedy, J., 1995. A new optimizer using particle swarm theory , 39–43.

Golmakani, H.R., Fazel, M., 2022. Constrained PSO for skewness-kurtosis portfolio models: An updated benchmark. Expert Systems with Applications 203, 117129.

Harvey, C.R., Siddique, A., 2020. Conditional skewness in asset pricing tests: Twenty-year retrospective. Journal of Finance 76, 1821–1852.

Jonsson, M., Rockinger, M., 2023. Moment component analysis in portfolio selection: A review. Journal of Banking & Finance 148, 106118.

Ledoit, O., Wolf, M., 2004. A well-conditioned estimator for large-dimensional covariance matrices. Journal of Multivariate Analysis 88, 365–411.

Ledoit, O., Wolf, M., 2008. Robust performance hypothesis testing with the sharpe ratio. Journal of Empirical Finance 15, 850–859.

Maringer, D., Parpas, P., 2009. Global optimization of higher order moments in portfolio selection. Journal of Global Optimization 43, 219–230.

Poli, R., Kennedy, J., Blackwell, T., 2007. Particle swarm optimization: An overview. Swarm Intelligence 1, 33–57.

Scott, R.C., Horvath, P.A., 1980. On the direction of preference for moments of higher order than the variance. Journal of Finance 35, 915–919.

Zhang, Y., Gong, D., Gao, X., 2020. Portfolio optimization based on multi-objective particle swarm optimization open architecture. Expert Systems with Applications 151, 113371.